Equilibrium and non-equilibrium controls on the abundances of clumped isotopologues of methane during thermogenic formation in laboratory experiments: Implications for the chemistry of pyrolysis and the origins of natural gases

Author links open overlay panel YanhuaShuai[ab] Peter M.J.Douglas[bc] ShuichangZhang[a] Daniel A.Stolper[d] Geoffrey S.Ellis[e] MichaelLawson[f] Michael D.Lewan[e] MichaelFormolo[f] JingkuiMi[a] KunHe[a] GuoyiHu[a] John M.Eiler[b]
Show more

https://doi.org/10.1016/j.gca.2017.11.024

Abstract

Multiply isotopically substituted molecules (‘clumped’ isotopologues) can be used as geothermometers because their proportions at isotopic equilibrium relative to a random distribution of isotopes amongst all isotopologues are functions of temperature. This has allowed measurements of clumped-isotope abundances to be used to constrain formation temperatures of several natural materials. However, kinetic processes during generation, modification, or transport of natural materials can also affect their clumped-isotope compositions. Herein, we show that methane generated experimentally by closed-system hydrous pyrolysis of shale or nonhydrous pyrolysis of coal yields clumped-isotope compositions consistent with an equilibrium distribution of isotopologues under some experimental conditions (temperature–time conditions corresponding to ‘low,’ ‘mature,’ and ‘over-mature’ stages of catagenesis), but can have non-equilibrium (i.e., kinetically controlled) distributions under other experimental conditions (‘high’ to ‘over-mature’ stages), particularly for pyrolysis of coal. Non-equilibrium compositions, when present, lead the measured proportions of clumped species to be lower than expected for equilibrium at the experimental temperature, and in some cases to be lower than a random distribution of isotopes (i.e., negative Δ_{18} values). We propose that the consistency with equilibrium for methane formed by relatively low temperature pyrolysis reflects local reversibility of isotope exchange reactions involving a reactant or transition state species during demethylation of one or more components of kerogen. Non-equilibrium clumped-isotope compositions occur under conditions where ‘secondary’ cracking of retained oil in shale or wet gas hydrocarbons($C_{2\text{-}5}$, especially ethane) in coal is prominent. We suggest these non-equilibrium isotopic compositions are the result of the expression of kinetic isotope effects during the irreversible generation of methane from an alkyl precursor. Other

interpretations are also explored. These findings provide new insights into the chemistry of thermogenic methane generation, and may provide an explanation of the elevated apparent temperatures recorded by the methane clumped-isotope thermometer in some natural gases. However, it remains unknown if the laboratory experiments capture the processes that occur at the longer time and lower temperatures of natural gas formation.

- **Previous** article in issue
- **Next** article in issue

Keywords

Thermogenic methane
Clumped isotopologues
Non-equilibrium
Coal
Shale

1. Introduction

Molecules containing two or more rare, heavy isotopes (multiply isotopically substituted molecules), known colloquially as ‘clumped isotopologues’ can be used as geothermometers (e.g., Ghosh et al., 2006, Came et al., 2007, Eiler, 2007, Guo, 2009, Eiler et al., 2014, Ono et al., 2014, Stolper et al., 2014a, Stolper et al., 2014b) due to their temperature-dependent enrichments relative to singly substituted and unsubstituted isotopologues of the same molecule in thermodynamically equilibrated systems (e.g., Urey and Rittenberg, 1933, Wang et al., 2004). It is also recognized that various physical, chemical and biochemical processescan lead to proportions of multiply substituted isotopologues different from those expected for equilibrium at the relevant environmental temperature (in some cases different from equilibrium at any temperature). Such non-equilibrium clumped-isotope effects in natural materials were first discussed for photochemical kinetic isotope effects expressed during the oxidation of atmospheric methane (Mroz et al., 1989, Kaye and Jackman, 1990). Non-equilibrium clumped-isotope effects have been documented in a variety of geochemical and biological processes including during isotope-exchange reactions and during the generation and destruction of carbonate minerals, CO_2, CH_4, C_2H_6, N_2O and O_2 (e.g., Eiler, 2007, Affek et al., 2008, Daëron et al., 2011, Passey and Henkes, 2012, Saenger et al., 2012, Clog et al., 2014, Stolper and Eiler, 2015, Stolper et al., 2015, Tripati et al., 2015, Wang et al., 2015, Wang et al., 2016, Yeung et al.,

2015, Douglas et al., 2017, Whitehill et al., 2017, Young et al., 2017). Such effects are not surprising given that many processes in nature, especially at near-surface temperatures (~25 °C), are controlled by kinetic as opposed to equilibrium processes. Non-equilibrium effects can be recognized when the measured temperature, based on the clumped-isotope temperature (i.e., the 'apparent' clumped-isotope temperature), is not the same as the known formation temperature of the molecule (though it should be recognized that kinetically controlled processes could fortuitously generate apparently equilibrated isotopic populations). In most previous studies where non-equilibrium clumped-isotope effects were observed, the materials in question formed at either known temperatures in the laboratory, or relatively well-constrained temperatures in nature. However, many geochemical problems (particularly those concerned with processes occurring in the Earth's interior) present situations in which materials of interest could have formed over a wide range of temperatures, making it challenging to evaluate whether a clumped-isotope temperature represents a real formation temperature, or the result of kinetic processes. Thermogenic methane presents such a problem because it can be generated by decomposition of organic matter over a wide range of temperatures (from 60 to over 250 °C) (e.g., Hunt, 1996). Recognized instances in which clumped-isotope thermometry agrees with other constraints on methane formation temperature, suggest that some thermogenic methane forms at isotopic equilibrium (Stolper et al., 2014a, Stolper et al., 2015, Stolper et al., in press, Wang et al., 2015, Young et al., 2017, Douglas et al., 2017). However, there are also examples for both biogenic and thermogenic gases where the measured methane clumped-isotope temperatures are either too high to be formation temperatures or negative Δ_{18} values are observed, which are not possible at isotopic equilibrium at any temperature (see below; Stolper et al., 2014b, Wang et al., 2015, Douglas et al., 2016, Young et al., 2017).

One explanation for clumped-isotope apparent temperatures of thermogenic methane formation that are too hot is that the gas formed out of isotopic equilibrium via kinetically controlled reactions. This situation might be expected given that the process of methane formation is generally described by kinetic rather than equilibrium controls on both chemical speciation and isotopic fractionation (e.g., Tang et al., 2000). Indeed, what is surprising is that in many natural settings it has been observed that thermogenic methane appears to form in or near isotopic equilibrium at environmental conditions (Stolper et al., 2014b, Stolper et al., 2015, Stolper et al., in press, Douglas et al., 2017). Herein, we explore the process of thermogenic methane formation with clumped-isotope analyses of methane produced by experimental nonhydrous pyrolysis of coal and

hydrous pyrolysis of shale. We evaluate the laboratory conditions under which clumped-isotope temperatures are consistent with formation temperatures and when they appear to be influenced by kinetic processes, and we discuss the possible relevance of these experimental findings to observations made previously on methane sampled from the environment.

2. Samples and experiments

Five separate series of pyrolysis experiments were conducted with different starting materials and procedures. The pyrolysis experiments each took immature organic-rich rocks (two marine shales and two coals) and heated them under different conditions (isothermal hydrous vs. nonhydrous heated at constant temperature ramp rates). Shale and coal are the two most common source rocks for natural gases, and hydrous conditions in stainless-steel reactors and nonhydrous conditions in gold tube vessels are the most common experimental systems used to simulate petroleum generation under laboratory conditions.

These experiments were designed to model the evolution of clumped isotopologues in thermogenic methane as a function of temperature and time. The temperature-time conditions of each of the experiments we present can be expressed as an equivalent 'maturity'—i.e., equivalent to a degree of time-at-temperature experienced by natural petroleum source rocks. It is common to express the maturity of natural hydrocarbon source rocks using the reflectance of vitrinite immersed in oil, reported as a percent 'R_o' value, which generally rises from values of ~0.5% at the onset of hydrocarbon generation to ~3.0% or slightly higher near the end of gas generation (roughly corresponding to temperatures of ~60–250 °C) (e.g., Hunt, 1996). We express the equivalent maturities of our heating experiments using the approximation Easy%Ro (the calculated Ro values using the algorithm of Burnham and Sweeney (1989)).

The following paragraphs summarize the materials and procedures of our five sets of experiments:

Coal I (experimental series 1 and 2): We performed nonhydrous pyrolysis of coal in sealed gold reactors (Table 1, Table 2) (Behar et al., 1992, Tang et al., 2000, Shuai et al., 2006). The first sample, termed Coal I, is a Tertiary lignite, collected from the Chuxiong coal mine in Yunnan province, southern China. The major composition and qualities as a petroleum source rock were determined using a Delsi-Nermag Rock-EvalIIPlus TOC analyzer. The sample has an H/C atomic ratio of 1.18, TOC (total

organic carbon concentration) of 48 wt%, HI (hydrogen index – hydrocarbon generation potential) of 132 mg HC/g TOC, T_{max}(temperature of maximum rate of hydrocarbon generation) of 423 °C, and R_o of 0.35%. Our experimental methods for this first coal sample involved loading 40 to 280 milligrams of crushed, dry coal (<80 mesh) into each of 21 gold reactors (40 mm × 4 mm i.d.), which were then sealed in an argon atmosphere and heated in a stainless-steel autoclave from 250 °C to a final temperature range of 300–620 °C at a specified rate (below), and then quenched in water immediately after reaching the designed final temperatures. Two separate heating rates were used: 10 °C/h or 1 °C/h. All experiments were conducted at 50 MPa pressure. Each heating schedule (i.e., the combination of rate and final temperature) was performed in duplicate simultaneously, with two gold vessels heated in one autoclave. A sample of gas was recovered from one of each of these paired experiments. Methane purified from each sample was analyzed for its $\delta^{13}C$, δD and clumped-isotopic composition (Δ_{18} value; see below) at the California Institute of Technology in Pasadena, following the methods of Stolper et al., 2014a, Stolper et al., 2014b (Table 1). The paired sample was analyzed for its gaseous molecular composition and yield (i.e., gaseous hydrocarbons, CO_2, H_2, H_2S) at the Key Laboratory of Organic Geochemistry of PetroChina in Beijing (Table 1). An external standard method was used to document a relative precision less than ±1 mol% for each component.

Table 1. Experimental conditions and measured values for natural gases produced by Yunnan Tertiary coal samples from Chuxiong mine, Yunnan province, southern China. (Coal I) in confined gold tubes without addition of water.

Heating rate	T	Easy%Ro	Gases yield (ml/g TOC)							CH_4						
			CH_4	C_2H_6	C_3H_8	C_{4+5}	H_2	CO_2	H_2S	δD (‰)	±	$\delta^{13}C$ (‰)	±	Δ_{18}(‰)	±	C (
10 °C/h	400	0.98	40.38	13.23	6.43	2.78	0.62	153.99	0.23	−313.80	0.15	−39.41	0.01	1.09	0.24	4
	420	1.19	55.47	18.14	8.55	4.15	0.74	170.51	0.20	−307.71	0.11	−38.72	0.00	1.13	0.22	4
	450	1.55	79.31	23.30	10.55	4.78	0.93	193.05	0.25	−300.57	0.11	−37.71	0.00	0.94	0.22	4
	480	2.01	105.02	25.96	10.60	3.04	1.26	208.46	0.14	−291.14	0.13	−36.49	0.01	0.97	0.24	4
	500	2.35	130.79	25.15	7.09	0.92	1.43	215.99	0.12	−281.78	0.14	−35.47	0.00	0.71	0.23	4
	520	2.71	151.15	22.67	4.01	0.41	1.55	219.64	0.07	−266.66	0.13	−34.35	0.01	0.19	0.24	9
	550	3.28	181.9	10.83	0.37	0.0	1.87	223.6		−243.21	0.13	−33.19	0.00	0.03	0.24	1

Heating rate	T	Easy%Ro	Gases yield (ml/g TOC)							CH_4						
			CH_4	C_2H_6	C_3H_8	C_{4+5}	H_2	CO_2	H_2S	δD (‰)	±	$\delta^{13}C$ (‰)	±	Δ_{18}(‰)	±	C (
			1			2		4								
	580	3.79	210.72	3.58	0.04	0.01	3.65	229.27		−199.36	0.11	−31.59	0.00	−1.51	0.24	n
	600	4.07	235.25	1.36	0.02	0.00	4.35	232.42		−172.40	0.11	−30.37	0.00	0.37	0.23	7
	620	4.31	256.34	1.28	0.01	0.00	6.18	235.22		−164.60	0.13	−29.71	0.00	0.43	0.24	6
1 °C/h	380	1.15	48.51	15.87	7.58	3.92	0.65	166.83	0.36	−316.19	0.13	−39.08	0.01	1.47	0.25	3
	400	1.39	62.71	19.56	9.96	4.85	0.73	181.86	0.36	−309.59	0.13	−38.00	0.01	1.22	0.20	3
	420	1.68	82.18	24.01	10.66	4.52	0.96	201.39	0.29	−303.73	0.11	−36.95	0.00	1.06	0.23	4
	440	2.01	108.23	25.64	9.97	3.05	1.12	209.26	0.21	−296.42	0.12	−35.94	0.00	1.02	0.24	4
	460	2.37	114.99	25.41	8.79	2.08	1.19	211.55	0.19	−292.05	0.14	−35.43	0.00	0.99	0.24	4
	480	2.76	151.86	20.62	2.53	0.40	1.61	219.48	0.12	−268.94	0.11	−33.64	0.00	0.11	0.24	9
	500	3.16	177.33	12.99	1.02	0.12	2.08	229.70		−242.73	0.12	−32.41	0.01	−0.30	0.24	n
	520	3.54	202.66	5.29	0.06	0.02	2.71	227.23		−203.66	0.13	−31.03	0.01	−0.84	0.24	n
	550	4.02	230.18	1.46	0.01	0.00	4.01	228.09		−178.28	0.12	−30.04	0.01	0.20	0.24	8
	580	4.39	257.13	0.64	0.01	0.00	6.20	237.27		−157.78	0.11	−28.71	0.00	0.74	0.25	5
	600	4.56	265.59	0.56	0.02	0.00	10.18	239.87		−145.83	0.12	−28.25	0.00	0.12	0.25	9

Notes: Values for $\delta^{13}C$, δD, and Δ_{18} reported relative to PDB, SMOW, and the stochastic distribution, respectively. Samples for which $\Delta_{18} \leq 0‰$ have no corresponding thermodynamically-allowed apparent equilibrium temperature.

Table 2. Experimental conditions and measured values for natural gases produced by CarboniferousChenjiashan coal samples from the Ordos Basin, China (Coal II) in confined gold tubes without addition of water (1 °C /h heating).

Sample	T	Easy%Ro	Gas yield (ml/g.TOC)			CH_4							
			CH_4	C_2H_6	C_3H_8	δD (‰)	±	$\delta^{13}C$ (‰)	±	Δ_{18}(‰)	±	Calc. T (°C)	±
Chenjiashan Coal	400	1.39	15.72	2.23	0.30								
	420	1.68	32.79	1.69	0.15	−277.59	0.13	−34.11	0.004	−0.12	0.22	no.data	no.data
	440	2.01	46.64	1.45	0.07	−260.06	0.12	−31.48	0.005	−0.17	0.24	no.data	no.data
	460	2.37	62.81	1.10	0.03	−246.17	0.12	−30.42	0.006	−0.33	0.26	no.data	no.data
	480	2.76	77.51	0.92	0.01	−190.32	0.13	−27.00	0.006	−0.64	0.27	no.data	no.data
	500	3.16	108.08	0.52	0.00	−165.78	0.12	−25.85	0.005	0.30	0.26	756	192

Notes: Values for $\delta^{13}C$, δD, and Δ_{18} reported relative to PDB, SMOW, and the stochastic distribution, respectively. Samples for which $\Delta_{18} \leq 0‰$ have no corresponding thermodynamically-allowed apparent equilibrium temperature.

Coal II (experimental series 3): A similar set of experiments was performed on a second, Carboniferous coal ('Coal II'), collected in the Chenjiashan coal mine in the Ordos Basin, central China. Coal II is less hydrogen-rich than Coal I, with an H/C ratio of 0.86. Additional characteristics for Coal II include: TOC = 48 wt%, HI = 139 mg HC/g TOC, T_{max} = 435 °C, and R_o = 0.52%. As for Coal I, aliquots of Coal II were loaded into gold tubes as described above and then heated to target temperatures ranging from 420 to 500 °C. Again, ramped heating was initiated at 250 °C. In this experiment, only one heating rate was used, 1 °C/h (Table 2). The molecular composition of the gas was determined and the methane was isolated and analyzed for its stable isotopic composition, including clumped-isotope composition (Table 2). We note that both the Coal I and II experiments were performed under conditions normally described as 'nonhydrous' but that structural water in the coal potentially was released during pyrolysis, and thus the experiments are not strictly nonhydrous. Nevertheless, no water was added to the samples for the coal experiments, unlike for the shale hydrous pyrolysis experiments described below.

Woodford Shale (Experimental series 4 and 5): Hydrous pyrolysis experiments on samples of the Woodford Shale (Upper Devonian to Lower Mississippian) were conducted using stainless-steel reactors at the U.S. Geologic Survey in Denver, following methods previously described (Lewan, 1983, Lewan, 1992, Lewan,

1993, Behar et al., 1995). Information pertaining to the characteristics of this organic-rich source rock can be found in Lewan (1983) and subsequent studies. The Woodford Shale I contains high organic matter concentrations with TOC of 27.3 wt.%, a HI value of 529 mg HC/g TOC, and a T_{max} of 425 °C. The Woodford Shale II has a TOC content of approximately 21 wt.%, a HI value of 423 mg HC/g TOC, and a T_{max} of 428 °C. The kerogen in both samples is predominantly Type-II with thermal maturity of approximately 0.4% R_o. The experiments on these materials involved isothermally heating ~200 g of gravel-sized (0.6–2.0 cm) shale with ~400 g of a 5 wt.% NaCl aqueous solution (to keep the aqueous phase subcritical at T > 374 °C) under a helium pressure of 6.9 MPa in a 1-liter reactor headspace (Lewan, 1993). The experiments were conducted at 330 °C (nominally bitumen and early oil generation), 360 °C (peak oil and gas generation), 390 °C (early oil cracking to wet gas), and 415 °C (late oil cracking and gas cracking to dry gas) for 72 h (Lewan, 1993). Gas samples were collected in 50-mL stainless-steel cylinders and analyzed for their molecular compositions at the U.S. Geologic Survey in Denver (Lewan, 1993) (Table 3). For Woodford Shale II, the expelled oil and residual kerogen were also collected, weighed and analyzed for composition after gas collection (Table 3). As was the case for the coal experiments, methane was purified and analyzed for its stable isotopic, including clumped isotope, composition (Table 3).

Table 3. Experimental conditions and measured values for natural gases produced by two samples of Upper Devonian – Lower Mississippian Woodford Shale (Shale II). Thermal maturity conditions for each experiment are expressed as equivalent vitrinite reflectance values (Easy%R_o) using the method of Burnham and Sweeney (1989).

Series	T (°C)	Easy%Ro	Gaseous composition (%)							Convertible Kerogen (mg/g.rock)	Bitumen (mg/g.rock)	Expelled Oil (mg/g.rock)	CH
			CH_4	C_2H_6	C_3H_8	C_{4+5}	H_2	CO_2	H_2S				δD
Woodford Shale I	330	0.89	15.40	8.60	4.44	2.56	4.21	60.73	3.08	n.a.	n.a.	n.a.	−33
	360	1.20	35.70	16.41	8.14	4.27	10.21	18.79	6.13	n.a.	n.a.	n.a.	−3
	390	1.59	49.89	11.98	5.84	3.18	10.90	15.05	2.82	n.a.	n.a.	n.a.	−3
Woodford Shale II	330	0.89	11.96	6.81	3.71	2.52	4.69	66.59	3.35	61.60	15.74	24.66	−3
	360	1.20	34.4	15.53	8.15	4.51	12.17	19.9	4.88	14.38	6.29	34.10	−3

Series	T (°C)	Easy%Ro	Gaseous composition (%)							Convertible Kerogen (mg/g.rock)	Bitumen (mg/g.rock)	Expelled Oil (mg/g.rock)	CH
			CH_4	C_2H_6	C_3H_8	C_{4+5}	H_2	CO_2	H_2S				δD
			0					0					
	390	1.59	48.06	11.71	6.05	3.86	11.37	15.82	2.79	5.07	4.80	13.13	−3
	415	2.00	56.69	8.94	4.71	2.10	11.58	15.85	0.04	0.91	0.44	n.a.	−3

n.a.: no analysis.

Note that all measurements of methane clumped-isotope composition reported herein are reported as 'Δ_{18}' values (Stolper et al., 2014a). Δ_{18} values represent the departure from a random isotopic distribution for the doubly substituted isotopologues, $^{13}CH_3D$ and $^{12}CH_2D_2$(Stolper et al., 2014a). $^{13}CH_3D$ makes up ~98% of the mass 18 methane isotopologues and dominates variations in Δ_{18} values for most isotopic fractionation processes. Δ_{18} values are reported as per mil (‰), where 0‰ refers to a random distribution of methane isotopologues. Due to an observed dependence of Δ_{18} on ^{18}R values, we applied heated gas correction using methane with different isotopic compositions equilibrated on a nickel catalyst at 500 °C, as detailed by Douglas et al. (2016).

3. Results

3.1. Evolution of clumped isotopologues of methane derived from coal

Methane generated during heating of Coal I at 10 °C/h at temperatures of 400 to 620 °C is characterized by Δ_{18} values ranging from −1.51‰ to + 1.13‰ (Table 1, Fig. 1; at temperatures less than 400 °C, insufficient methane was produced for clumped-isotopic analysis). Methane generated at temperatures between 400 and 500 °C from this series have Δ_{18} values consistent with formation at equilibrium with Δ_{18} values of 1.13 to 0.71 per mil with respect to homogeneous isotope exchange reaction among methane isotopologues at the experimental temperature. It is perhaps significant that the methane recovered from these experiments actually formed over a range of temperatures less than or equal to the designed, final temperature; i.e., gas is generated continuously during the heating schedule and accumulates from the start of the experiment up until each designed temperature. Methane recovered from experiments at temperatures of 520 to 600 °C yielded Δ_{18} values that departed from

predicted equilibrium by more than 2 standard errors of the measurement, in all cases falling to Δ_{18} values lower than expected for equilibrium. Indeed, in some cases Δ_{18} values are lower than 0‰. Negative Δ_{18} values (sometimes described as an 'anti-clumped' distribution) do not correspond to any apparent formation temperature, as Δ_{18} values are >0‰ for all finite temperatures for an equilibrated system. Negative Δ_{18}values have been observed previously only in biogenic (or presumed biogenic) methane (Stolper et al., 2015, Wang et al., 2015, Douglas et al., 2016, Young et al., 2017). Δ_{18} values depart furthest from equilibrium at 520 °C, suggesting a sharp transition from equilibrium to non-equilibrium Δ_{18} values as temperature rises from 500 to 520 °C (see Fig. 1). Above 520 °C, Δ_{18} values rise, approaching the expected equilibrium composition, and falling within 1 standard error of equilibrium by 620 °C.

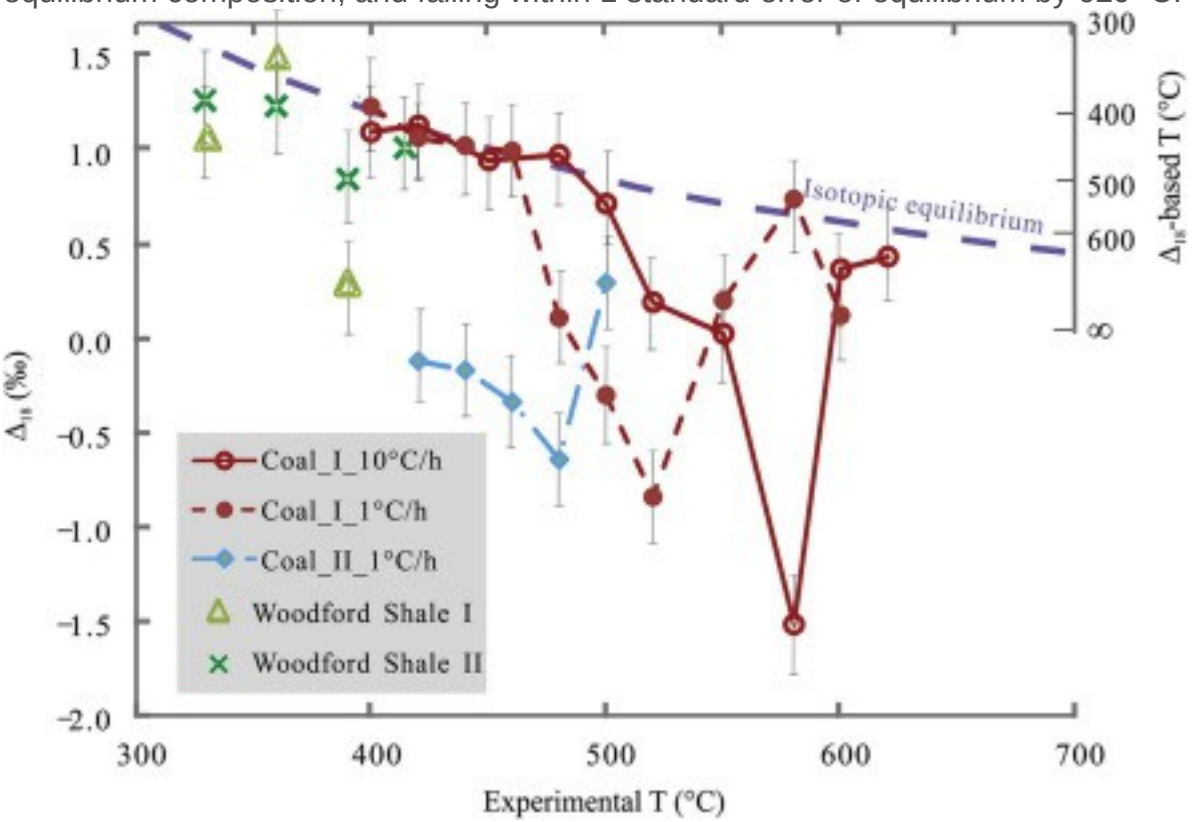

1. Download high-res image (140KB)
2. Download full-size image

Fig. 1. Plot of the Δ_{18} value (in ‰, relative to a stochastic distribution) of methane produced by coalnonhydrous pyrolysis or shale hydrous pyrolysis experiments, vs. the experimental temperature. The dashed line shows the calibrated trend of Δ_{18} vs. temperature consistent with thermodynamic equilibrium(Stolper et al., 2014a, Stolper et al., 2014b). The trends of Δ_{18} variation with temperature differ between the experimental series, but are homologous. Δ_{18} is generally consistent with equilibrium

among methane isotopologues (particularly for the three best sampled temperature-series—Coal I at 1 and 10 °C/h, and the second, more detailed Woodford Shale experiments). Further heating leads to departures from equilibrium, to lower Δ_{18} values (in some cases falling below 0). The highest temperature experiments on coals show a return toward (in some cases reaching) equilibrium.

The general pattern of Δ_{18} evolution with increasing temperature is reproduced by the second set of Coal I experiments, where the heating rate was 1 °C/h as opposed to 10 °C/h: Methane recovered from experiments in which Coal I was heated at 1 °C/h varies in Δ_{18} from +1.47‰ to −0.84‰ (Table 1). These samples follow a pattern of values consistent with formation in isotopic equilibrium at relatively low temperature (380–460 °C), depart from equilibrium to lower than expected Δ_{18} values at temperatures of 480–550 °C —including Δ_{18} values less than 0— and return toward Δ_{18} values consistent with equilibrium as the final temperature of the experiment rises to ≥580 °C (Fig. 1).

The two experimental series described above were conducted, purified and analyzed months apart, suggesting that their similar pattern of evolution in Δ_{18} reflects a phenomenon of methane production as opposed to an artifact associate with sample storage, preparation or measurement. Specifically, the series that was heated at 10 °C/h was performed in January 2015 and purified and measured in September to October 2015, whereas the series involving heating at a 1 °C/h rate was conducted in November to December 2015 and purified and analyzed in February to March 2016.

It is significant that the 1 °C/h experimental series produces a pattern of Δ_{18} variations with temperature that resembles that for the 10 °C/h series, but that the non-equilibrium signature starts at a lower temperature of 480 °C for the slower heating rate (vs. 520 °C for fast heating), and approaches within 1 sigma error of equilibrium at a lower temperature of 580 °C (vs. 600–620 °C). When experimental temperatures are converted to thermal maturities (presented herein as Easy%R_o values following Burnham and Sweeney (1989), we find that departures from equilibrium are associated with a particular range in thermal maturity rather than a temperature, per se, becoming most marked at calculated values of 2.5% R_o (Fig. 2). This finding suggests that the pattern of Δ_{18} variation could reflect isotope effects associated with the overall progress of kerogen and hydrocarbon ‘cracking’ reactions.

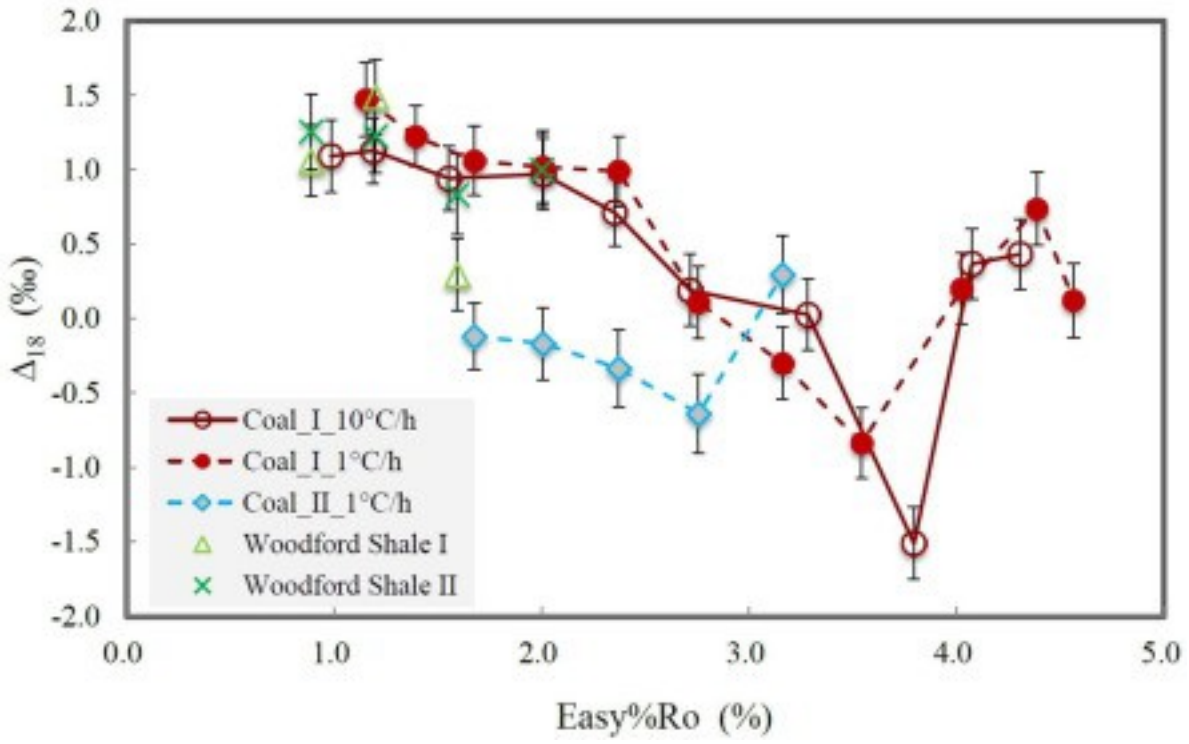

1. Download high-res image (103KB)
2. Download full-size image

Fig. 2. Plot of methane Δ_{18} value (in ‰, relative to a stochastic distribution) vs. equivalent vitrinite reflectance (Easy%R_o) calculated according to Burnham and Sweeney (1989).

It is not straightforward to translate this finding into a prediction of the maturities of natural sources at which this phenomenon might occur. The maturity index used here (Easy%R_o) is calculated for the high temperatures (330–620 °C) and short times (hours to days) of our experiments. Comparable %R_o values in natural kerogens would be generated at far lower temperatures (60 to over 250 °C) and longer times (millions to tens of millions of years). However, further insight into the controls of non-equilibrium Δ_{18} values in these experiments can be found by plotting the Δ_{18} value of methane vs. gas wetness (the proportion of non-methane alkanes in the gas fraction; Fig. 3). In such a plot, data from these two coal pyrolysis experimental series define similar ‘V’-shaped trends (Fig. 3). That is, Δ_{18} coevolves with similar trends when plotted vs. properties of gas chemistry that depend on overall thermal maturity, regardless of the heating rate and temperature at which a given thermal maturity is reached (and, as will be shown below, regardless of differences in pyrolysis substrate).

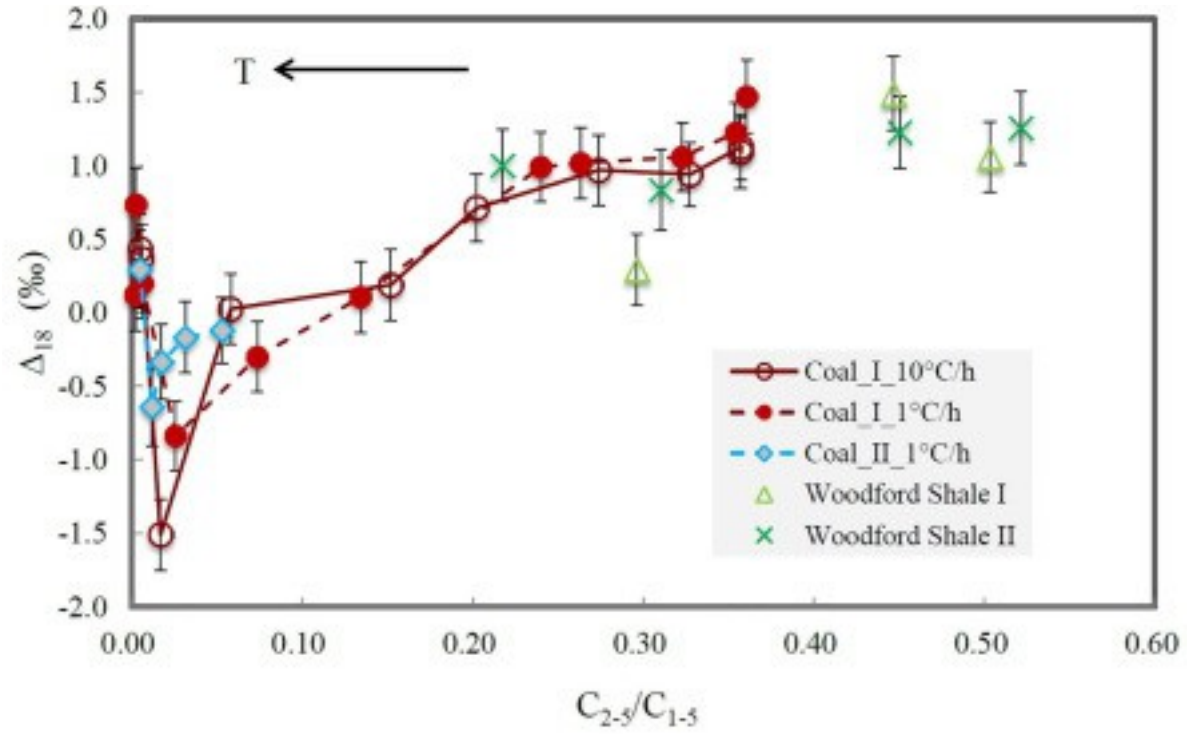

1. Download high-res image (111KB)
2. Download full-size image

Fig. 3. Plot of methane Δ_{18} value (in ‰, relative to a stochastic distribution) vs. the 'wetness' of the coexisting gas phase, where wetness is defined as the molar ratio: C_{2-5}/C_{1-5}. Note that despite the fact that the various coal and shale experimental series follow trends that are homologous but offset in temperature in Fig. 1, all experimental series conform to a single pattern in Fig. 3. Δ_{18} of methane is consistent with equilibrium during early generation of wet gas, but drops precipitously to non-equilibrium values as gas wetness decreases, and then sharply returns toward equilibrium in the highest temperature, driest gases.

The smaller set of pyrolysis experiments conducted on Chenjiashan coal (Coal II) produces methane with non-equilibrium Δ_{18} values from −0.64‰ to +0.30‰ at maximum experimental temperatures between 420 and 500 °C, all reached at heating rates of 1 °C/h (Table 2). Only one experiment exhibits a Δ_{18} value that approaches the expected Δ_{18} value for the final temperature point—the experiment ending at 500 °C (Δ_{18} = 0.3‰ ± 0.26, 1 s.e., which is within two standard errors of the expected value at 500 °C, 0.81‰). This series of experiments has too few data points to determine conclusively whether it reinforces the findings for the two series of experiments on Coal I (other than confirming that it is possible to generate non-equilibrium, even negative Δ_{18} values by coal pyrolysis). However, the pattern of variation of Δ_{18} values for products of Coal II pyrolysis are at least consistent with those for the Coal I series. Most significantly, the

Coal II experiments conform to the pattern of Coal I experiments in Fig. 3, where Δ_{18} of methane is plotted vs. gas wetness. This suggests that all three experimental series exhibit a common control on Δ_{18} values, related to other features of gas chemistry, but that Coal II reaches the stage of non-equilibrium methane production at somewhat lower $\%R_o$ values than does Coal I. That is, non-equilibrium Δ_{18} values are always associated with the interval of thermal maturity where wet gas components first diminish in abundance, most obviously marked by strong decreases in ethane and propane yields (Fig. 4c; Table 2). Moreover, the stage where non-equilibrium methane is first observed corresponds to a change in the rate of increase of δD values of methane with rising temperature (Fig. 4b), and to a change in the slope in a plot of the $\delta^{13}C$ value of methane versus the maximum experimental temperature (Fig. 5, Fig. 6). These findings suggest that the H and C isotope fractionations associated with methane production change at the same point in the heating history when the Δ_{18} value of methane changes.

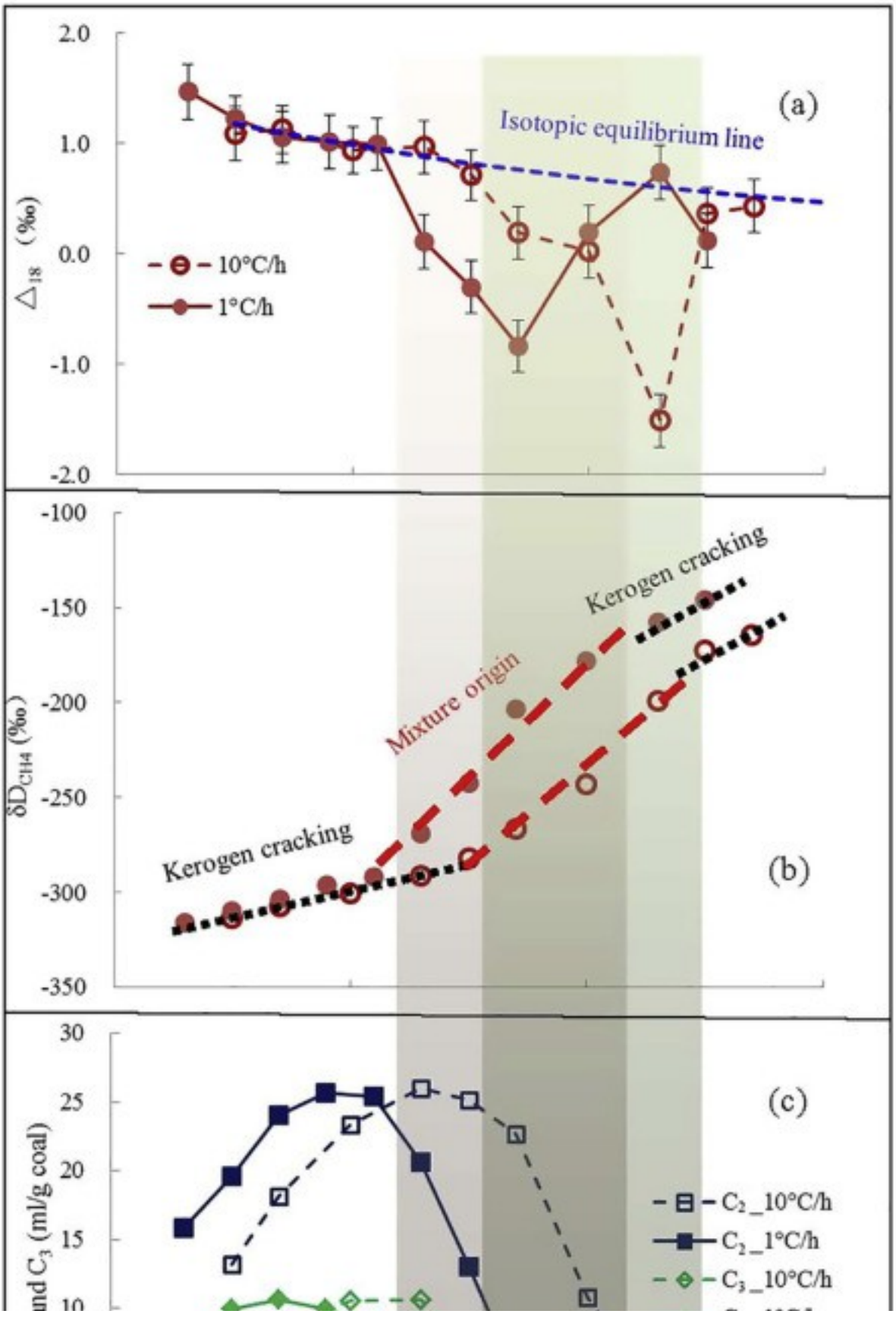
2.0
1.0
0.0
-1.0
-2.0
Δ_{18} (‰)
(a)
Isotopic equilibrium line
10°C/h
1°C/h
-100
-150
-200
-250
-300
-350
δD_{CH4} (‰)
Kerogen cracking
Mixture origin
Kerogen cracking
(b)
30
25
20
15
10
nd C_3 (ml/g coal)
(c)
C_2_10°C/h
C_2_1°C/h
C_3_10°C/h

1. Download high-res image (218KB)
2. Download full-size image

Fig. 4. Variation in methane stable isotope compositional indices and gas chemistry with increasing pyrolysis temperature in Yunnan coal (I) pyrolysis experiments. (a) Δ_{18} values; note the non-equilibrium values are observed at lower temperatures in the 1 °C/h heating experiments compared to the 10 °C/h heating experiments. (b) δD values; note rate of rise in δD with increasing temperature changes in the same temperature interval where non-equilibrium Δ_{18} values are seen (c) The relative yields of ethane to propane; note the dramatic decrease in ethane yield in the same temperature interval where non-equilibrium methane Δ_{18} values are observed.

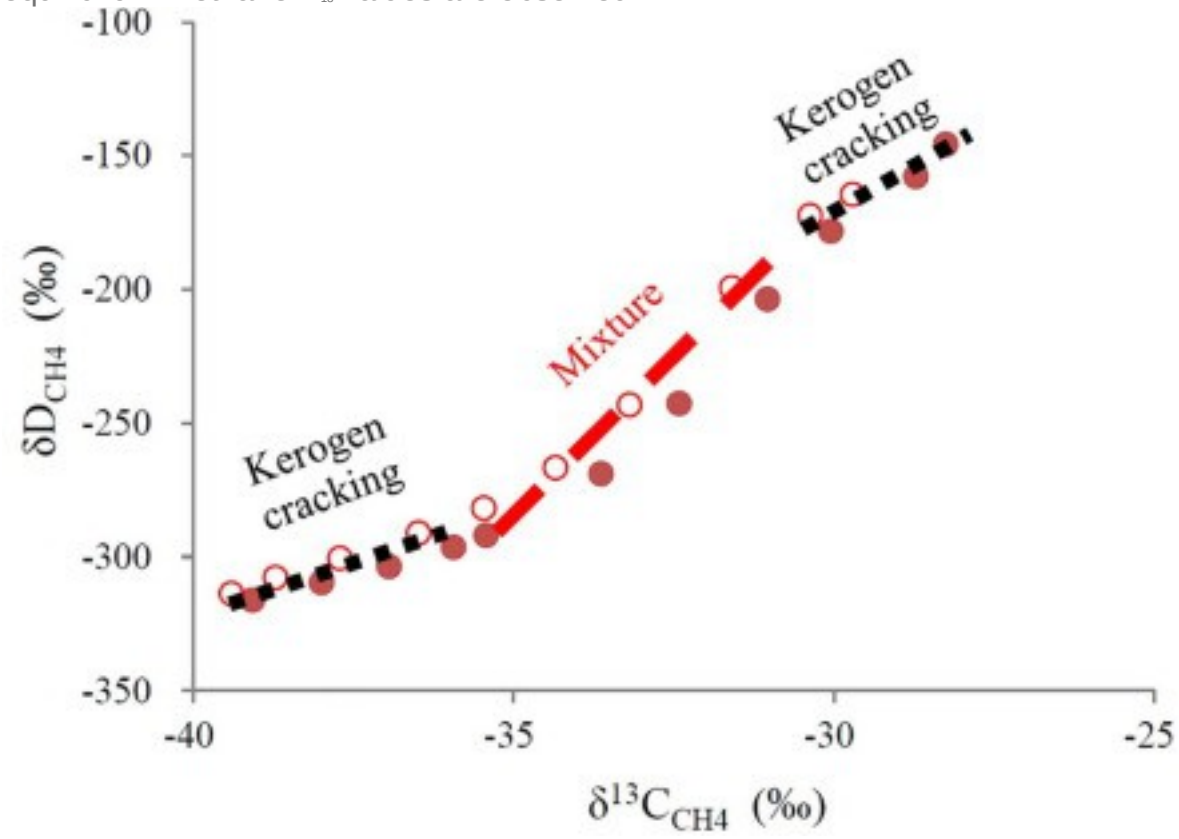

1. Download high-res image (73KB)
2. Download full-size image

Fig. 5. A plot of δD_{CH4} and $\delta^{13}C_{CH4}$ values of methane from coal I. Change in the isotopic fractionationfactor between product methane and source organic matter could reflect production of methane from different methane precursors at different temperatures. Formation of methane with non-equilibrium clumped-isotope compositions occurs when the slope in this plot changes.

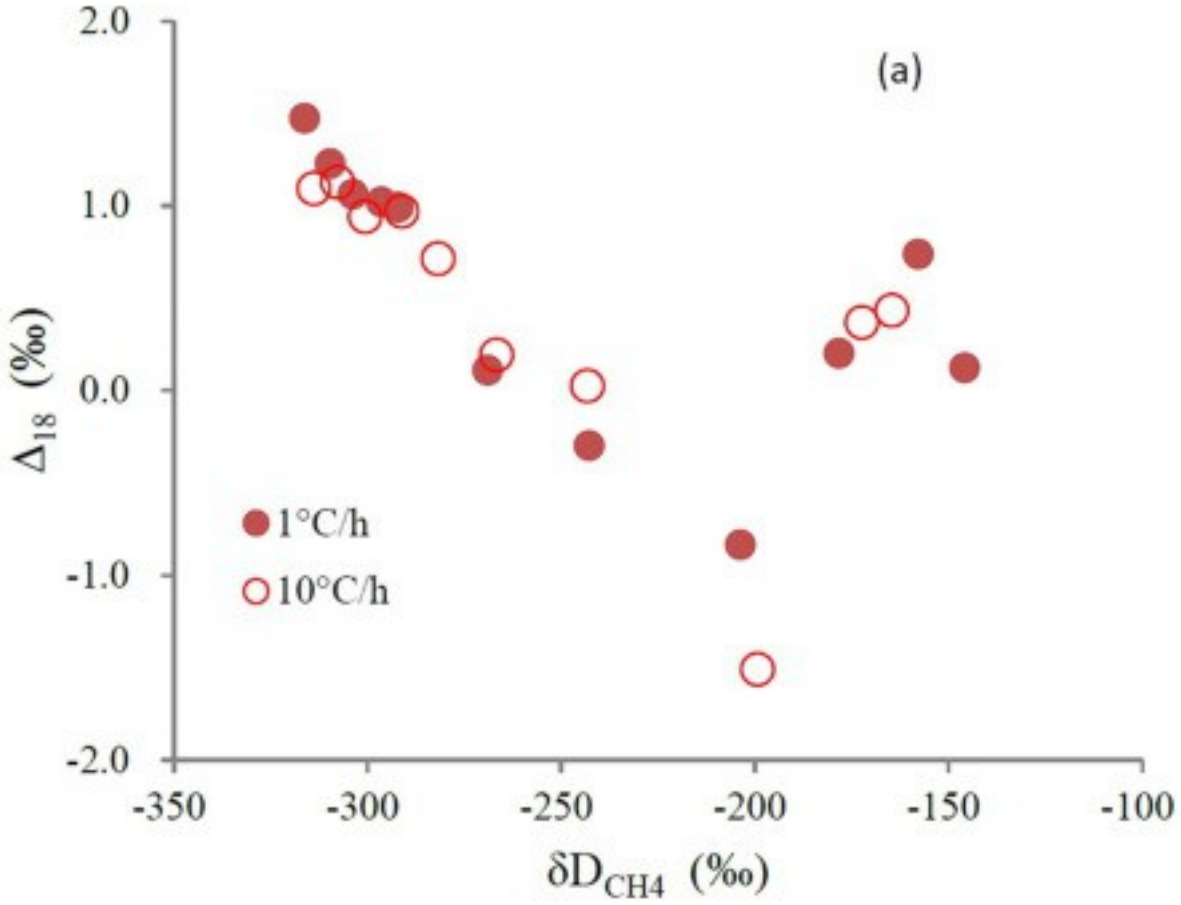
(a)
2.0
1.0
0.0
-1.0
-2.0
Δ_{18} (‰)
1°C/h
10°C/h
-350
-300
-250
-200
-150
-100
δD_{CH4} (‰)

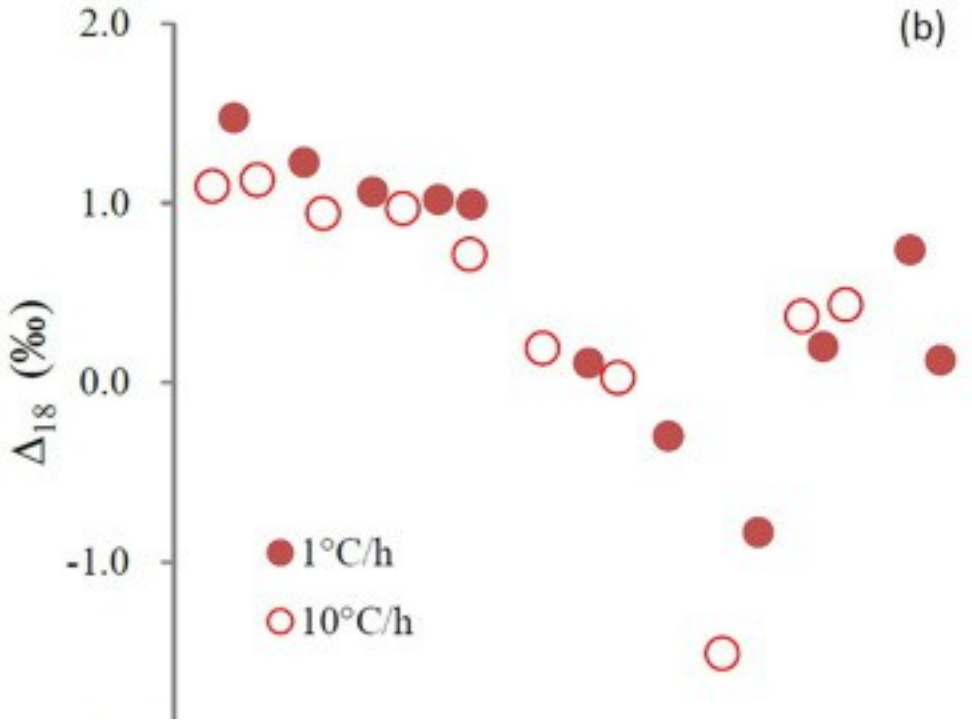
(b)
2.0
1.0
0.0
-1.0
Δ_{18} (‰)
1°C/h
10°C/h

1. Download high-res image (121KB)
2. Download full-size image

Fig. 6. The plots of δD_{CH4} vs. Δ_{18} and $\delta^{13}C_{CH4}$ vs. Δ_{18}. The Δ_{18} value of methane coevolves with the δD_{CH4} value along a single trend despite variations in heating rate (1 °C/h or 10 °C/h) (a), and a similar finding is observed when Δ_{18} is plotted vs. $\delta^{13}C_{CH4}$ value (b).

3.2. Clumped isotopologues of methane derived from shale

The two series of experiments in which the Woodford Shale was subjected to hydrous pyrolysis at 330 to 415 °C yielded methane with Δ_{18} values ranging from +1.49‰ to +0.3‰ (Fig. 1, Table 3). Unlike the coal pyrolysis experiments, most Woodford Shale experiments yield methane with Δ_{18} values within analytical errors of equilibrium at the conditions of the experiment; only experiments at 390 °C (a temperature at which oil cracking begins) fall to lower Δ_{18} values, suggesting some form of non-equilibrium fractionation. While the Δ_{18}values observed in these two sets of experiments are not identical, they generally follow the same trend with increasing temperature: a relatively close approach to equilibrium at 330 and 360 °C; a small departure from equilibrium at 390 °C (the deviation from equilibrium is particularly noticeable at 390 °C in Shale I); and a return to Δ_{18} values consistent with formation in equilibrium at 415 °C (observed only for Shale II because no experiment was conducted at this temperature for Shale I). Thus, the shale pyrolysis experiments roughly follow the pattern observed in coal pyrolysis, but with a smaller overall range in Δ_{18}, and with departures from equilibrium observed at lower temperatures and equivalent source maturities (Fig. 1, Fig. 2). However, the departure from equilibrium Δ_{18} values in the experiments with oil-prone source rocks seems to be associated with cracking of liquid hydrocarbons (Table 3), whereas in coal pyrolysis this phenomenon is associated with dramatic losses of wet gas components (Table 1, Table 2).

4. Discussion

We focus our discussion on the two principal findings of this study:
(1) methane produced by shale and coal pyrolysis is in, or closely approaches, equilibrium with respect to its Δ_{18}values over significant ranges of relatively low and very high temperatures, yet (2) the same substrates yield methane with substantial departures from equilibrium at intermediate temperatures, coincident with the onset of destruction of wet gas and/or oil components. Both of these results present challenges to our understanding of the chemistry of pyrolytic methane generation.

4.1. The relationship between Δ_{18} values and inferred methane formation mechanisms

Thermogenic methane can be generated from a variety of organic precursors including kerogen, bitumen, oil, and wet gases (C_{2-5}) (Fig. 7). These differ in their relative contributions to the produced methane, as a function of the type of organic matter present, how open the source rock is to loss of hydrocarbons, and the thermal maturity of the source rock (e.g., Tissot et al., 1974, Behar et al., 1995, Behar et al., 1997, Hunt, 1996, Cramer, 2004). It is important to note that the process of petroleum generation from any specific precursor occurs over a restricted thermal maturity range (e.g., oil window); however, these ranges typically overlap at least partially (Fig. 7).

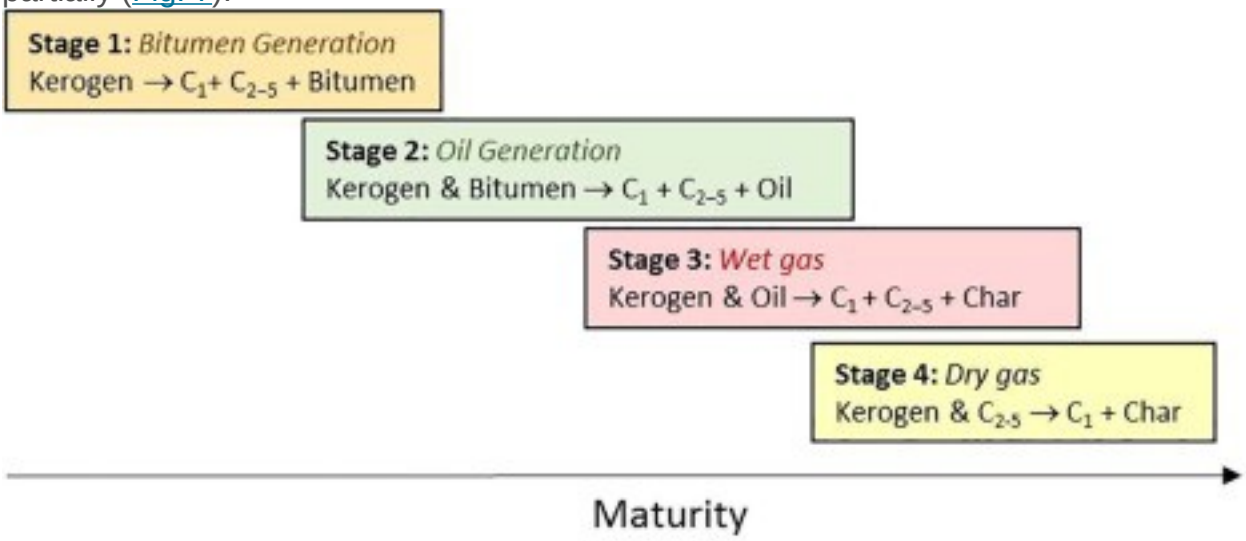

1. Download high-res image (65KB)
2. Download full-size image

Fig. 7. Conceptual scheme for petroleum generation in the pyrolysis experiments conducted for this study. Kerogen and bitumen are operationally defined as the fractions of organic matter that are insoluble and soluble, respectively, in common organic solvents. Char (or pyrobitumen) is a solid organic carbonresidue that is hydrogen poor. Note that the stages of petroleum generation are not mutually exclusive.

The initial stage of catagenesis (Stage 1, Fig. 7) involves the partial transformation of solid organic matter that is insoluble in organic solvents (kerogen) to a mobile, organic phase that is enriched in high-molecular weight and heteroatomic (N, S, and O) containing organic molecules (bitumen) (Tissot et al., 1974, Behar et al., 1995, Behar et al., 1997, Hunt, 1996, Cramer, 2004). This occurs over temperatures of 65 to 95 °C in typical source rocks exposed to geological heating rates, and the earliest formed thermogenic methane is associated with this process (Tissot et al., 1974, Hunt, 1996). Further thermal evolution of organic-rich rocks leads to the transformation of bitumen to a liquid petroleum phase that can be expelled from the source rock (oil) (Stage 2, Fig.

7). Compared to the first stage of petroleum generation the second stage produces significantly larger amounts of natural gas and these gases contain higher concentrations of C_{2-5} alkanes (ethane through pentane; e.g., Behar et al., 1995, Behar et al., 1997, Cramer, 2004). Following methane production by kerogen and bitumen transformation to oil and gas, additional methane is generated by the cracking of liquid hydrocarbons (Stage 3, Fig. 7). Further temperature increases can result in the thermal cracking of wet gas components (C_{2-5}) into methane (Stage 4, Fig. 7). Because the substrates undergoing cracking are the products of primary generation processes associated with kerogen decomposition, this phase (Stages 3 and 4, Fig. 7) is sometimes referred to as 'secondary cracking' (Tissot et al., 1974). At the highest thermal maturities, a final phase of kerogen rearrangement and cracking is possible that results in pure methane production.

Methane formation by kerogen cracking/rearrangement is believed to be dominated by demethylation from complex organic structures and breaking of heteroatomic bonds, whereas that generated during liquid hydrocarbon or wet gas cracking is believed to result mainly from breaking C–C bonds of aliphatic hydrocarbons such as n-alkanes (Tissot et al., 1974, Behar et al., 1995, Behar et al., 1997, Hunt, 1996, Cramer, 2004). Finally, we note that the kinetics of methane clumped-isotope re-equilibration are believed to be slow (even over geological timescales) at temperatures up to ~200–250 °C (Wang et al., 2015), but are not well known and may be significant at higher temperatures—perhaps even fast enough for laboratory timescale re-equilibration at the temperatures of pyrolysis experiments (300–600 °C).

One interpretation of our findings, in particular the 'V'-shaped patterns of Δ_{18} variation in Fig. 2, Fig. 3, is that thermogenic methane formed by demethylation of kerogen precursors is locally reversible (i.e., hydrogen is rapidly exchanged between the methyl group or the transition state structure into which it is incorporated and nearby sites) and therefore produces methane that is in or near a clumped-isotope equilibrium. This suggestion may be reinforced by the relatively gentle rise in δD_{CH4} with increasing maturity for methane generated during these stages (i.e., because the exchangeable pool of hydrogen atoms at least partially buffers any rise in δD; Fig. 5). Furthermore, we suggest that cracking of alkyl precursors instead involves irreversible reactions and kinetic isotope effects that lead to methane deviating from clumped-isotope equilibrium. In the case of coal pyrolysis, this alkyl precursor could be ethane, propane, other gas components, or alkyl side chains in aromatic compounds. We suspect ethane cracking as a possible source of methane having a non-equilibrium Δ_{18} value, as the largest drop in Δ_{18} values during the coal pyrolysis experiments occurs at the temperatures

corresponding to a sharp drop in the yield of ethane (Fig. 4c, Table 1, Table 2). In the case of the Woodford Shale hydrous pyrolysis experiments, some components in the bitumen and/or oil could serve the same role in the temperature step when departures from equilibrium are observed (390 °C; Table 3). Note that coal is gas-prone whereas shale is oil-prone under their respective pyrolysis conditions (Tissot et al., 1974, Behar et al., 1995, Hunt, 1996, Seewald, 2003). The products of pyrolysis of coal lack the significant liquid yields that are generated during shale pyrolysis, so cracking of oil compounds is unlikely to be prevalent during pyrolysis of coals. One observation that reinforces this interpretation is our finding that the hydrogen isotopic composition of methane evolves more rapidly with increasing temperature in the range where Δ_{18} most strongly deviates from equilibrium (Fig. 4b). It is also plausible that this change in reaction mechanism is responsible for the shift in the trend of δD_{CH4} and $\delta^{13}C_{CH4}$ values over the temperature range in question (Fig. 5), suggesting a change in the associated fractionationfactor between methane and its precursor(s), and/or different isotopic compositions of the precursors (Cramer, 2004).

Our finding of Δ_{18} values far from equilibrium up to 580 °C suggests that re-equilibration of methane (i.e., reversible isotopic exchange after methane has formed) is not effective on laboratory timescales in the presence of coal, shale and/or water, at least up to these temperatures. However, it is imaginable that the return toward equilibrium Δ_{18} values at the highest experimental temperatures reflects re-equilibration, either instead of, or in addition to, the methane production from kerogen rearrangement that we suggest above. Understanding these exchange kinetics will require experiments designed to measure the rate constants for methane isotopic re-equilibration under a variety of conditions. However, one feature of our findings argues against re-equilibration as a significant factor in our experiments: The temperature at which Δ_{18} begins to rise back toward equilibrium in Fig. 1differs by heating rate and substrate, from 500 °C for slow heating of Coal II, to 550 °C for slow heating of Coal I, to 600 °C for fast heating of Coal I. This behavior is consistent with control by reaction progress of primary or secondary cracking reactions, and is not expected for simple isotopic redistribution among methane molecules (though it is possible that some combination of pre-exponential factors and activation energies for such exchange reactions could be consistent with our data). An additional factor that may influence the rise in Δ_{18}values at the highest experimental temperatures is that the latest stages of methane production from alkyl precursors (i.e., secondary gas and oil cracking) will draw on a pool of reactants that is residual to extensive prior to pyrolysis. If those pyrolysis reactions preferentially extract methane with low Δ_{18} values, it is possible that the residue becomes correspondingly

enriched in ^{13}C–D bonds and thus yields methane with higher Δ_{18} values at the highest extents of heating. Such fractionation effects are important to the interpretation of H and C isotope compositions of petroleum compounds (Cramer, 2004). We consider this process in more detail in Section 4.3.

4.2. Alternate hypotheses for the origins of non-equilibrium Δ_{18} values in thermogenic methane

4.2.1. Mixing?

Thermogenic methane is frequently a mixture of components generated from different substrates, and from reactions at different conditions; this is clearly true in our pyrolysis experiments and is often true in nature. For example, during the early phases of catagenesis (Stages 1 and 2, Fig. 7), both kerogen and bitumen can react to generate methane (Hunt, 1996). Thus, even methane generated from a single source rock at a single temperature, pressure, and time should be thought of as a mixture of products from different precursors. In the case of our experiments, methane sampled at the end of each experiment was generated over a range of temperatures, and in some cases is suspected to be a mixture of methane produced from kerogen and methane produced from an alkyl precursor (wet gas components in our coal pyrolysis experiments and bitumen or oil in our shale pyrolysis experiments).

Mixing is capable of disturbing clumped-isotope compositions for two reasons. Most obviously, two fractions of methane that form in equilibrium, but at different temperatures, will differ in their Δ_{18} values, and their mixture will create a gas having some intermediate Δ_{18}value that does not reflect either temperature of methanogenesis. This phenomenon likely contributes to some of Δ_{18} variations observed in this study, but is not of primary importance because it cannot be solely responsible for the most extreme non-equilibrium clumped-isotope compositions we observe. However, a second mixing phenomenon is of greater possible interest. In a population of methane molecules having a random distribution of ^{13}C and D among all isotopologues, the proportions of $^{13}CH_3D$ and $^{12}CH_2D_2$ generally vary non-linearly with changes in $\delta^{13}C$ and δD (Douglas et al., 2017, Young et al., 2017). As a result, in a mixture of two gases that are identical in Δ_{18} value, but differ in $\delta^{13}C$ and/or δD, the Δ_{18}value of their mixture could differ from that of the end member components. This phenomenon is common to all of the clumped-isotope systems studied to date, and has been explored by theory, experiments and natural samples in several previous papers (see Eiler, 2013, for a review). Such mixing led to methane formed through oil biodegradationhaving Δ_{18} values higher than those expected from equilibrium (Douglas et al., 2017). However, there is

good reason to conclude that this cannot be responsible for non-equilibrium Δ_{18} values observed in our experiments. The products of both coal pyrolysis and shale hydrous pyrolysis exhibit positive correlations between all pairs of $\delta^{13}C$, δD and temperature. Thus, mixtures of gases generated at higher and lower temperatures should always involve mixing lower-$\delta^{13}C$, lower-δD methane with higher-$\delta^{13}C$, higher-δD methane. Such mixing processes should always lead to increases in the Δ_{18} values of the mixtures relative to the weighted average of the Δ_{18} of the end member components. Thus, it seems impossible that mixing produced lower than equilibrium (much less negative) Δ_{18} values. The only caveat we note is that it is imaginable that the bulk $\delta^{13}C$ and δD values of methane observed in our experiments reflect combinations of a high-$\delta^{13}C$, low-δD and low-$\delta^{13}C$, high-δD end member (a mixing scenario that can lead to low Δ_{18} values), and that through some fortuitous control of the proportions of these end members, this never manifests as a departure from the general evolution from low to high $\delta^{13}C$ and δD with increasing temperature and reaction progress. Nevertheless, this scenario strikes us as exceptionally implausible, and we conclude that mixing plays no significant role in producing the non-equilibrium Δ_{18} values we observe.

4.2.2. Methane produced by reaction of carbon compounds with H_2?

Although kerogen and hydrocarbon cracking reactions are likely to dominate the isotopic compositions of methane in our experiments, there is also the potential that an exogenous source of hydrogen (i.e., an inorganic source of hydrogen not associated with the kerogen or derived products of cracking) could also be incorporated into methane. Microbial methanogenesis in the presence of high partial pressures of molecular hydrogen have been shown to give rise to non-equilibrium signatures in methane generated both in the laboratory and in shallow lakes and sediments (Stolper et al., 2015, Wang et al., 2015, Douglas et al., 2016). While the conditions and mechanisms of these biologically mediated reactions differ greatly from those in the experiments presented herein, this provides at least an example of non-equilibrium Δ_{18} values arising from irreversible H additions to carbon (though note that in our case these reactions are associated with rising methane δD, whereas in biosynthesisthey are associated with very low δD). Herein, we observe no clear correlation between Δ_{18}values and H_2 concentration in any of the pyrolysis experiments (Table 1, Table 3). Instead, H_2 concentrations (and partial pressure) slowly increase with increasing temperatures in all experiments, and exhibit no deviation in the rate of accumulation as methane signatures first deviate toward non-equilibrium compositions. Thus, no circumstantial evidence suggests that non-equilibrium Δ_{18} values in thermogenic methane produced in this study reflect reactions involving H_2.

4.2.3. Methane produced by water reduction?

Another alternative hypothesis worth considering is that thermogenic methane that exhibits a non-equilibrium clumped-isotope composition is a product of the reaction of water with a carbon-bearing substrate (Lewan, 1993, Seewald, 2003). Such a process can occur both via the reduction of oxidized forms of carbon (relative to C in methane) such as graphite, CO_2, and CO with electrons derived, in some cases, from water, and via the reaction of hydrocarbons with water to produce shorter chain carbon compounds that incorporate water-derived hydrogen and oxygen (Seewald, 2003). It is worth considering whether methane produced by this mechanism might be responsible for departures from the apparently typical thermogenic pattern of near-equilibrium Δ_{18} values toward lower values. One might argue against this possibility based on the fact that one of our experimental series involved hydrous pyrolysis, whereas the other was nominally nonhydrous, yet both have a temperature interval over which methane forms out of isotopic equilibrium. Indeed, the difference between nonhydrous and hydrous pyrolysis experiments presented herein suggests that if water has any effect, it is to reduce the amplitude of the non-equilibrium Δ_{18}signature. On the other hand, some amount of water is likely present in the coal pyrolysis experiments, adsorbed or otherwise contained in the organic precursors. So, it is possible aqueous reactions occurred in these experiments as well. It is not obvious why such a reaction would occur over a narrow temperature range of 50–100 °C and then (apparently) stop with further heating, as implied by the return to equilibrium in our highest temperature experiments. Additionally, it is difficult to understand why the role of the water would occur at different temperatures for different heating rates and starting sedimentary rock compositions, yet still maintain correlations with gas composition. For these reasons, we consider it possible but unlikely that non-equilibrium methane formed by some process involving reaction of water with other components of the experimental systems.

4.2.4. Kinetic isotope fractionations during cracking of kerogen moieties rather than oil and gas components?

Another alternative interpretation to our suggestion in Section 4.1 is that a non-equilibrium Δ_{18} value for thermogenic methane is associated with a particular kerogen cracking mechanism (i.e., rather than cracking an oil or gas alkyl compound, as proposed above). This mechanism could be particular to radical decomposition (β scission) of some class of kerogen moieties having unsaturated C to produce methane only at a specific maturity:

(1)$RCH_3CH{\cdot}CH_3 \rightleftharpoons CH_{3\bullet} + RCH = CH_2$

One plausible example is the homolytic cleavage of alkyl groups from the beta-position of aromatic molecules (e.g., Xiao, 2001):
(2)
These alkyl groups become progressively enriched in coals with maturation, and are also abundant in bitumen (Xiao, 2001). Unlike other cracking reactions, there is no meta-stable transition state involved in the homolytic cleavage, and therefore this reaction mechanism could more likely give rise to non-equilibrium isotopic fractionations. In contrast, the breakdown of kerogen (or oil) through radical decomposition pathways (Eq. (3)) and hydrogen transfer reactions (Eq. (4)), are perhaps more likely to generate equilibrium methane by locally reversible transfer of hydrogen atoms between hydrocarbon transition states and/or positions within reactant and/or product molecules.
(3)$RCH_3 \rightleftharpoons CH_{3\bullet} + R_\bullet$
(4)$R + CH_{3\bullet} \rightleftharpoons CH_4 + R_\bullet$
We believe this hypothesis is worth further exploration, but note that it does not provide a good explanation as to why the non-equilibrium methane in coal pyrolysis corresponds to the temperature range where ethane is destroyed by secondary gas cracking, because such alkyl-rich material is expected to be monotonically enriched in coal with maturation.

If we are correct to suggest that alkyl cracking is responsible for forming thermogenic methane with non-equilibrium Δ_{18} values, then the most dramatic example of this phenomenon encountered in this study seems to be ethane cracking during advanced stages of coal pyrolysis. Additional and more targeted experiments will be required to resolve whether and how such a kinetic isotope effect might arise during ethane cracking. However, we suggest the following factors are a plausible starting hypothesis. Thermogenic methane formation involves the production of methyl radicals as intermediates, which combine with one H to form methane. A kinetic isotope effect could be associated either with formation of the methyl radical state, or with H addition to that radical. If the observed overall kinetic isotope effect were partly or entirely due to conversion of ethane to a methyl radical intermediate, we might expect a buildup of ^{13}C-D and D-D substituted ethane in the residue, to compensate for the production of a methyl radical pool having a deficit in $^{13}CH_2D_\bullet$ and $^{12}CHD_{2\bullet}$. As the conversion of ethane to methane progresses to high overall extents of reaction, we might expect that this buildup of doubly substituted reactant ethane will eventually drive the proportion of $^{13}CH_2D_\bullet$ and $^{12}CHD_{2\bullet}$ intermediates (and thus $^{13}CH_3D$ and $^{12}CH_2D_2$ products) up. That is,

mass balance constraints suggest that any kinetic isotope effect that is expressed at the beginning of ethane cracking will eventually return to a net methane product composition close to equilibrium. This phenomenon could explain why the Δ_{18} value of methane drops at the onset of ethane cracking and then returns to higher (near equilibrium) values as ethane is almost completely consumed. However, there is no correlation between the magnitude of the deviation from the expected equilibrium value and the extent of the reaction (such as ethane cracking) that produces the non-equilibrium methane. The magnitude of the non-equilibrium signal is possibly a combined effect of other factors. For example, it should be related to the proportion of the non-equilibrium methane in the total methane (e.g., the contribution from ethane cracking in our coal pyrolysis experiments). Further studies will be needed to investigate other possible factors and their exact influence.

4.3. Non-equilibrium Δ_{18} values in methane from natural gases

Whatever mechanisms are responsible for the non-equilibrium generation of clumped isotopologues of thermogenic methane, an important question remains as to whether natural systems that make such methane follow the equilibrium mechanism we associate with kerogen cracking or rearrangement, or the non-equilibrium mechanism we associate with alkyl cracking, or some combination of these two mechanisms. It seems plausible that our findings could be mirrored by variations in the Δ_{18} of natural thermogenic methane. On the other hand, the non-equilibrium phenomenon we observe experimentally appears to occur only over a relatively narrow range of temperatures, at temperatures hundreds of degrees above those typical of natural petroleum-generating systems, and for the nonhydrous experiments, at heating rates ~10 orders of magnitude higher than in nature. Also, whether the same mechanism of wet gas cracking occurs in nature as in our experiments is unclear. Consequently, it is not clear whether the observed non-equilibrium phenomena could occur in natural systems.

There is evidence for the generation of thermogenic methane both in and out of clumped-isotope equilibrium in nature. First, the 100+ clumped-isotope measurements made to date of natural, nominally thermogenic, methane include many examples where Δ_{18}-based apparent temperatures are consistent with independent constraints on their geological origins (Stolper et al., 2014b, Stolper et al., 2015, Stolper et al., in press, Douglas et al., 2017, Shuai et al., in press). This was first demonstrated by Stolper et al. (2014b) where methane produced from the Marcellus and Haynesville Shales had clumped-isotope temperatures that were within uncertainty of those estimated from independent geological constraints. A subsequent study of natural gases from the Antrim Shale containing mixtures of biogenic and thermogenic gases

reached similar conclusions (Stolper et al., 2015). There is additional evidence that migrated thermogenic gases from conventional gas deposits often have Δ_{18} values consistent with thermogenic formation temperatures in the deeper, petroleum forming portions of their respective basins. Examples of these basins include the Potiguar Basin samples examined by Stolper et al. (2014b); as well as numerous samples of this kind from coastal Brazil, the Gulf of Mexico, the North Sea and continental Europe (Rotliegend), all reported in Douglas et al. (2017) and discussed further in Stolper et al. (in press). We further illustrate this common finding by presenting new clumped-isotope measurements of methane from three dry ($C_1/C_{1\text{-}5}$ >0.99) shale gases from unconventional deposits of the Silurian Longmaxi Shale (Type II organic matter) with % R_o values of 2.2% to 3.1% in the Sichuan Basin, southern China (e.g., Liu et al., 2014). These gases yielded Δ_{18}-based temperatures in the range ~167 to 206 °C—consistent with independent estimates of the corresponding temperatures of their source rocks (Table 4). Taken together, these data strongly suggest that the equilibrium we observe early and late in coal and shale pyrolysis (argued herein to reflect phases of kerogen cracking and rearrangement) is a common feature of natural thermogenic methane formation.

Table 4. Molecular and stable isotopic composition, including clumped isotopes of methane, for produced shale gases from the Sichuan Basin, China.

Location	Well	Gas composition (%)				$\delta^{13}C$ (‰,PDB)			CH_4							
		CO_2	N_2	CH_4	C_2H_6	C_1	C_2	CO_2	δD (‰)	±	$\delta^{13}C$ (‰)	±	Δ_{18}(‰)	±	Calc. T (°C)	±
Sicuan Basin	J-1	1.16	0.47	97.67	0.68	−30.8	−35.3	0.8	−140.95	0.14	−30.37	0.005	3.09	0.24	162	17
	W-1	1.01	0.43	98.17	0.39	−35	−38.5	−1.5	−134.04	0.13	−35.54	0.004	2.62	0.23	199	20
	W-2	8.45	2.17	89.32	0.06	−32.5	−33.4	2.7	−136.02	0.13	−33.02	0.005	2.55	0.25	206	22

On the other hand, recent studies of natural thermogenic methane have also revealed cases in which the Δ_{18}-based apparent temperature is significantly greater than the maximum temperature that seems plausible based on independent geological or geochemical constraints. Unconventional oil accumulations in both the Eagle Ford Shale and Bakken Formation (Douglas et al., 2017) produce gas associated with oil that have methane Δ_{18}values with apparent temperatures in excess of 200 °C. As oil stability is generally assumed to be lower than 200 °C on geological time frames (e.g., Tissot et al., 1974, Seewald, 2003), the temperatures are unlikely to represent the geological conditions of petroleum generation. Furthermore, the methane in these systems has low

$\delta^{13}C_{PDB}$ values, from −38 to −47‰, generally associated with oil-window thermal maturities. These facts suggest methane in these systems was generated from source rocks that reached the oil window or wet gas window (maturity index values of % R_0 = 1.1 to 1.8), but no higher (Berner and Faber, 1996). There are several possible explanations for this discrepancy, but one that is suggested by the experimental results presented here is that part of the methane in these shale oilaccumulations comes, entirely or in part, from 'secondary' cracking which starts from % Ro > 1.3 (e.g., Tissot et al., 1974, Hunt, 1996), or, as we discuss in Section 4.2.4, the occurrence of the homolytic cleavage from the beta position of an aromatic compound. It is noteworthy that the Eagle Ford Shale and Bakken Formation systems are the only unconventional oil shales to be subject to significant methane clumped-isotope study so far, and thus it is possible this non-equilibrium signature is a distinctive geochemical signature of such settings.

5. Summary and conclusions

The methane generated by nominally nonhydrous pyrolysis of coals and hydrous pyrolysis of Woodford Shale exhibits clumped-isotope compositions (Δ_{18} values) that are consistent with equilibrium for parts of the temperature ranges explored, but non-equilibrium compositions for other portions of the experimental temperature ranges. The association of non-equilibrium clumped-isotope signatures with temperature intervals when bitumen, oil or wet gas components undergo secondary cracking lead us to suggest that methane generated during kerogen cracking and/or rearrangement forms in or near clumped-isotope equilibrium (perhaps due to locally reversible exchange of hydrogen), whereas alkyl cracking (of bitumen, oil or wet gases components) is an irreversible process that manifests kinetic isotope effects on the clumped-isotope composition. Studies of natural thermogenic methanes suggest both of these mechanisms could operate in natural hydrocarbon systems, with equilibrium kerogen cracking dominating the methane found in dry, unconventional shale gases and conventional oil and gas deposits, and the non-equilibrium (alkyl cracking?) process dominating methane found as a dissolved component in unconventional shale oils.

Acknowledgements

This work was cosponsored by the NSFC (41772135), NSTMP (2016ZX05007-01) and PetroChina Foundation (2017ycp014); analyses of Woodford Shale gases are either taken from Stolper et al. (2014b) or newly measured for this study as part of a continuing research collaboration supported by ExxonMobil. Any use of trade, firm, or

product names is for descriptive purposes only and does not imply endorsement by the U.S. government. We thank Dr. Hagit Affek, Dr. Shuhei Ono, Dr. Robert Dias, and two anonymous reviewers for their valuable comments and suggestions.

References

Affek et al., 2008

H.P. Affek, M. Bar-Matthews, A. Ayalon, A. Matthews, J.M. Eiler**Glacial/interglacial temperature variations in Soreq cave speleothems as recorded by 'clumped isotope' thermometry**

Geochim. Cosmochim. Ac., 72 (22) (2008), pp. 5351-5360

ArticleDownload PDFView Record in Scopus

Behar et al., 1992

F. Behar, S. Kressmann, J.L. Rudkiewicz, M. Vandenbroucke**Experimental simulation in a confined system and kinetic modelling of kerogen and oil cracking**

Org. Geochem., 19 (1) (1992), pp. 173-189

ArticleDownload PDFView Record in Scopus

Behar et al., 1997

F. Behar, M. Vandenbroucke, Y. Tang, F. Marquis, J. Espitalie**Thermal cracking of kerogen in open and closed systems: determination of kinetic parameters and stoichiometric coefficients for oil and gas generation**

Org. Geochem., 26 (5) (1997), pp. 321-339

ArticleDownload PDFView Record in Scopus

Behar et al., 1995

F. Behar, M. Vandenbroucke, S.C. Teermann, P.G. Hatcher, C. Leblond, O. Lerat**Experimental simulation of gas generation from coals and a marine kerogen**

Chem. Geol., 126 (3) (1995), pp. 247-260

ArticleDownload PDFView Record in Scopus

Berner and Faber, 1996

U. Berner, E. Faber**Empirical carbon isotope/maturity relationships for gases from algal kerogens and terrigenous organic matter, based on dry, open-system pyrolysis**

Org. Geochem., 24 (10–11) (1996), pp. 947-955

ArticleDownload PDFView Record in Scopus

Burnham and Sweeney, 1989

A.K. Burnham, J.J. Sweeney**A chemical kinetic model of vitrinite maturation and reflectance**

Geochim. Cosmochim. Ac., 53 (1989), pp. 2649-2657

ArticleDownload PDFView Record in Scopus

Came et al., 2007

R.E. Came, J.M. Eiler, J. Veizer, K. Azmy, U. Brand, C.R. Weidman**Coupling of surface temperatures and atmospheric CO_2 concentrations during the Palaeozoic era**

Nature, 449 (7159) (2007), pp. 198-201
CrossRefView Record in Scopus

Clog et al., 2014

M.D. Clog, A.A. Ferreira, E.V. Santos Neto, J.M. Eiler**Ethane C-C clumping in natural gas: a proxy for cracking processes?**
AGU Fall Meeting Abstracts, vol. 1 (2014), p. 06
View Record in Scopus

Cramer, 2004

B. Cramer**Methane generation from coal during open system pyrolysis investigated by isotope specific, Gaussian distributed reaction kinetics**
Org. Geochem., 35 (4) (2004), pp. 379-392
ArticleDownload PDFView Record in Scopus

Daëron et al., 2011

M. Daëron, W. Guo, J. Eiler, D. Genty, D. Blamart, R. Boch, R. Drysdale, R. Maire, K.Wainer, G. Zanchetta**$^{13}C^{18}O$ clumping in speleothems: Observations from natural caves and precipitation experiments**
Geochim. Cosmochim. Ac., 75 (12) (2011), pp. 3303-3317
ArticleDownload PDFView Record in Scopus

Douglas et al., 2017

P. Douglas, D. Stolper, J. Eiler, A. Sessions, A. Bishop, M. Lawson, Y. Shuai, D. Valentine, J. Fiebig, A. Luhrmann, G. Etiope, M. Schoel, N. Kitchen**Clumped isotopes in methane: Progress and potential for a new isotopic tracer**
Org. Geochem. (2017), 10.1016/j.orggeochem.2017.07.016

Douglas et al., 2016

P.M. Douglas, J. Stolper, D.A. Smith, K.W. Anthony, C.K. Paull, S. Dallimore, M. Wik, P.M.Crill, M. Winterdah, J.M. Eiler, A.L. Sessions**Diverse origins of Arctic and Subarctic methane point source emissions identified with multiply-substituted isotopologues**
Geochim. Cosmochim. Ac., 188 (2016), pp. 163-188
ArticleDownload PDFView Record in Scopus

Eiler, 2007

J.M. Eiler**“Clumped-isotope” geochemistry—The study of naturally-occurring, multiply-substituted isotopologues**
Earth Planet. Sc. Lett., 262 (3) (2007), pp. 309-327
ArticleDownload PDFView Record in Scopus

E
i
l

e
r
.
2
0
1
3

J.M. Eiler**The isotopic anatomies of molecules and minerals**
Annu. Rev. Earth Planet. Sci., 41 (2013), pp. 411-441
CrossRefView Record in Scopus

Eiler et al., 2014

J.M. Eiler, B. Bergquist, I. Bourg, P. Cartigny, J. Farquhar, A. Gagnon, W. Guo, A. Hofmann, T.E. Larson, N. Levin, E.A. Schauble, D. Stolper**Frontiers of stable isotope geoscience**
Chem. Geol., 372 (2014), pp. 119-143
ArticleDownload PDFView Record in Scopus

Ghosh et al., 2006

P. Ghosh, J. kins, H. Affek, B. Balta, W. Guo, E.A. Schauble, D. Schrag, J.M. Eiler^{13}**C–**^{18}**O bonds in carbonate minerals: A new kind of paleothermometer**
Geochim. Cosmochim. Ac., 70 (6) (2006), pp. 1439-1456
ArticleDownload PDFView Record in Scopus

Guo, 2009

W. Guo**Carbonate clumped isotope thermometry: application to carbonaceous chondrites and effects of kinetic isotope fractionation**
PhD thesis
California Institute of Technology (2009)

Hunt, 1996

J. Hunt**Petroleum Geology and Geochemistry**
Freeman and Company press, New York (1996)

Kaye and Jackm

J.A. Kaye, C.H. Jackman**Comment on “Detection of multiply deuterated methane in the atmosphere”**
Geophys. Res. Lett., 17 (1990), pp. 659-660
CrossRefView Record in Scopus

Lewan, 1983

M.D. Lewan**Effects of thermal maturation on stable organic carbon isotopes as determined by hydrous pyrolysis of Woodford shale**
Geochim. Cosmochim. Ac., 47 (8) (1983), pp. 1471-1479
ArticleDownload PDFView Record in Scopus

Lewan, 1992

M. Lewan**Water as a source of hydrogen and oxygen in petroleum formation by hydrous pyrolysis**
Am. Chem. Soc. Div. Fuel Chem., 37 (1992), pp. 1643-1649
View Record in Scopus

Lewan, 1993

M. Lewan**Laboratory simulation of petroleum formation**
Org. Geochem. (1993), pp. 419-442
Springer
CrossRef

Liu et al., 2014

S.G. Liu, B. Ran, X.L. Guo, S.Q. Wang, Q.H. Hu, Y. Luo**From Oil-prone Source Rock to Gas-producing Shale Reservoir: Lower Palaeozoic Organic-matter-rich Black Shale in the Sichuan Basin and its Periphery**
Science Press, Beijing (2014)
(In Chinese with English abstract)

Mroz et al., 1989

E.J. Mroz, M. Alei, J.H. Cappis, P.R. Guthals, A.S. Mason, D.J. Rokop**Detection of multiply deuterated methane in the atmosphere**
Geophys. Res. Lett., 16 (1989), pp. 677-678
CrossRef

Ono et al., 2014

S. Ono, D.T. Wang, D.S. Gruen, Lolla
B. Sherwood, M.S. Zahniser, B.J. McManus, D.D. Nelson**Measurement of a doubly substituted methane isotopologue, $^{13}CH_3D$, by tunable infrared laser direct absorption spectroscopy**
Anal. Chem., 86 (13) (2014), pp. 6487-6494
CrossRefView Record in Scopus

Passey and Hen

B.H. Passey, G.A. Henkes**Carbonate clumped isotope bond reordering and geospeedometry**
Earth Planet. Sc. Lett., 351 (2012), pp. 223-236
ArticleDownload PDFView Record in Scopus

Saenger et al., 2

C. Saenger, H.P. Affek, T. Felis, N. Thiagarajan, J.M. Lough, M. Holcomb**Carbonate clumped isotope variability in shallow water corals: Temperature dependence and growth-related vital effects**

Geochim. Cosmochim. Ac., 99 (2012), pp. 224-242
ArticleDownload PDFView Record in Scopus

Seewald, 2003

J.S. Seewald**Organic–inorganic interactions in petroleum-producing sedimentary basins**
Nature, 426 (6964) (2003), pp. 327-333
CrossRefView Record in Scopus

Shuai et al., 200

Y. Shuai, P.A. Peng, Y. Zou, S.C. Zhang**Kinetic modeling of individual gaseous component formed from coal in a confined system**
Org. Geochem., 37 (8) (2006), pp. 932-943
ArticleDownload PDFView Record in Scopus

Shuai et al., in pr

Shuai Y., Etiope G., Zhang S., Douglas P., Huang L. and Eiler J. (in press) Methane clumped isotopes in the Songliao Basin (China): New insights into abiotic vs. biotic hydrocarbon formation. *Earth Planet. Sci. Lett.*, http://doi.org/10.1016/j.epsl.2017.10.057.

Stolper et al., 20

D.A. Stolper, A.L. Sessions, A.A. Ferreira, E.S. Neto, A. Schimmelmann, S.S. Shusta, D.L.Valentine, J.M. Eiler**Combined 13C–D and D-D clumping in methane: Methods and preliminary results**
Geochim. Cosmochim. Ac., 126 (2014), pp. 169-191
ArticleDownload PDFView Record in Scopus

Stolper et al., 20

D. Stolper, M. Lawson, C.L. Davis, A.A. Ferreira, E.S. Neto, G.S. Ellis, M.D. Lewan, A.M.Martini, Y. Tang, M. Schoell, A.L. Sessions, J.M. Eiler**Formation temperatures of thermogenic and biogenic methane**
Science, 344 (6191) (2014), pp. 1500-1503
CrossRefView Record in Scopus

Stolper et al., 20

D.A. Stolper, A.M. Martini, M. Clog, P.M. Douglas, S.S. Shusta, D.L. Valentine, A.L. Sessions, J.M. Eiler**Distinguishing and understanding thermogenic and biogenic sources of methane using multiply substituted isotopologues**
Geochim. Cosmochim. Ac., 161 (2015), pp. 219-247
ArticleDownload PDFView Record in Scopus

Stolper and Eiler

D.A. Stolper, J.M. Eiler**The kinetics of solid-state isotope-exchange reactions for clumped isotopes: A study of inorganic calcites and apatites from natural and experimental samples**
Am. J. Sci., 315 (5) (2015), pp. 363-411
CrossRefView Record in Scopus

Stolper et al., in

Stolper D. A., Lawson M., Formolo M. and Eiler J. M. (in press) The utility of methane clumped isotopes to constrain the origins of methane in natural gas accumulations. *Geol. Soc. London.*

Tang et al., 2000

Y. Tang, J. Perry, P.D. Jenden, M. Schoell**Mathematical modeling of stable carbon isotope ratios in natural gases**
Geochim. Cosmochim. Ac., 64 (15) (2000), pp. 2673-2687
ArticleDownload PDFView Record in Scopus

Tissot et al., 197

B. Tissot, B. Durand, J. Espitalie, A. Combaz**Influence of nature and diagenesis of organic matter in formation of petroleum**
AAPG Bull., 58 (3) (1974), pp. 499-506
View Record in Scopus

Tripati et al., 201

A.K. Tripati, P.S. Hill, R.A. Eagle, J.L. Mosenfelder, J. Tang, E.A. Schauble, J.M. Eiler, R.E.Zeebe, J. Uchikawa, T.B. Coplen, J.B. Ries, J.B. Ries**Beyond temperature: Clumped isotope signatures in dissolved inorganic carbon species and the influence of solution chemistry on carbonate mineral composition**
Geochim. Cosmochim. Ac., 166 (2015), pp. 344-371
ArticleDownload PDFView Record in Scopus

Urey and Rittenb

H.C. Urey, D. Rittenberg**Some thermodynamic properties of the H_1H_2, H_2H_2 molecules and compounds containing the H_2atom**
J. Chem. Phys., 1 (2) (1933), pp. 137-143
CrossRefView Record in Scopus

Wang et al., 201

D.T. Wang, D.S. Gruen, B.S. Lollar, K.U. Hinrichs, L.C. Stewart, J.F. Holden, A.N. Hristov, J.W.Pohlman, P.L. Morrill, M. Konneke, K.B. Delwiche, E.P. Reeves, C.N. Sutcliffe, D.J. Ritter, J.S. Seewald, J.C. McIntosh, H.F. Hemond, M.D. Kubo, D. Cardace, T.M. Hoehler, K.B. Delwiche**Nonequilibrium clumped isotope signals in microbial methane**
Science, 348 (6233) (2015), pp. 428-431
CrossRefView Record in Scopus

Wang et al., 201

D.T. Wang, P.V. Welander, S. Ono**Fractionation of the methane isotopologues $^{13}CH_4$, $^{12}CH_3D$, and $^{13}CH_3D$ during aerobic oxidation of methane by Methylococcus capsulatus (Bath)**
Geochim. Cosmochim. Ac., 192 (2016), pp. 186-202
ArticleDownload PDFView Record in Scopus

Wang et al., 200

Z. Wang, E.A. Schauble, J.M. Eiler**Equilibrium thermodynamics of multiply substituted isotopologues of molecular gases**
Geochim. Cosmochim. Ac., 68 (23) (2004), pp. 4779-4797
ArticleDownload PDFView Record in Scopus

Whitehill et al., 2

A.R. Whitehill, L.M.T. Joelsson, J.A. Schmidt, D.T. Wang, M.S. Johnson, S. Ono**Clumped-isotope effects during OH and Cl oxidation of methane**
Geochim. Cosmochim. Ac., 196 (2017), pp. 307-325
ArticleDownload PDFView Record in Scopus

Xiao, 2001

Y.T. Xiao**Modeling the kinetics and mechanisms of petroleum and natural gas generation: a first principles approach**
Rev. Mineral. Geochem., 42 (1) (2001), pp. 383-436
CrossRefView Record in Scopus

Yeung et al., 201

L.Y. Yeung, J.L. Ash, E.D. Young**Biological signatures in clumped isotopes of O_2**
Science, 348 (6233) (2015), pp. 431-434
CrossRefView Record in Scopus

Young et al., 201

E.D. Young, I.E. Kohl, B.S. Lollar, G. Etiope, D. Rumble, S. Li, M.A. Haghnegahdar, E.A.Schauble, K.A. McCain, D.I. Foustoukos, C. Sutclife, O. Warr, C.J. Ballentine, T.C. Onstott, H.Hosgormez, A. Neubeck, J.M. Marques, I. Perez-Rodriguez, A.R. Rowe, D.E. Larowe, C. Magnabosco, L.Y. Yeung, J.L. Ash, L.T. Bryndzia**The relative abundances of resolved $^{12}CH_2D_2$ and $^{13}CH_3D$ and mechanisms controlling isotopic bond ordering in abiotic and biotic methane gases**
Geochim. Cosmochim. Ac., 203 (2017), pp. 235-264
ArticleDownload PDFView Record in Scopus